

Investigation of the $\text{CH}_3 + \text{NO}$ Reaction in Shock Waves

G. Hennig and H. Gg. Wagner

Institut für Physikalische Chemie Göttingen, Tammannstraße 6, D-37077 Göttingen, Germany

Key Words: Chemical Kinetics / Elementary Reactions / Radicals / Shock Waves / Spectroscopy (Infrared)

The reaction of $\text{CH}_3 + \text{NO}$ was investigated behind incident shock waves at temperatures between 1300 K and 2080 K. The formation of H atoms and of HCN was studied by time resolved UV absorption and by IR-emission. OH measurements of Hoffmann et al. were reevaluated with the rate constant of this work. The rate constant for the reaction of $\text{CH}_3 + \text{NO}$ can be expressed by

$$k = (4.0 \pm 0.8) \cdot 10^{12} \exp(-8500 \pm 500 \text{ K}/T) \text{ cm}^3 \text{ mol}^{-1} \text{ s}^{-1}.$$

HCN was found to be the main final product of the reaction of $\text{CH}_3 + \text{NO}$ in the temperature range covered. The contribution of the H forming channels is around 20–25% to the main channel.

Introduction

In combustion processes of hydrocarbons in air NO is an unwanted but hardly avoidable by-product. There are several hydrocarbon radicals in flames like CH or CH_2 which can react with NO and break the N–O bond respectively replace it by a C–N bond. This is offering a chance for the nitrogen to end up as N_2 . A hydrocarbon radical which is present in combustion processes in rather high concentrations is CH_3 and its reaction with NO is therefore of some interest.

The rate constant for the reaction of CH_3 with NO was measured by several authors (see e.g. [1]). Near room temperature the reaction proceeds as recombination reaction forming CH_3NO and it should show the typical recombination reaction behaviour with regard to pressure and temperature dependence of the rate constant. The formation of other products requires an activation energy. There is a rather large number of possible reaction channels respectively products which may be formed in that reaction (see [2]).

In addition to the investigations mentioned [1] there are some recent experiments about the rate of the reaction of $\text{CH}_3 + \text{NO}$ at different temperatures.

Titarchuk et al. [3] determined the rate constant from pyrolysis of $[(\text{CH}_3)_3\text{CO}]_2$ with NO in a flow circulation system directly from the formation of CH_3NO at pressures between 30–270 mbar. They obtained a value for the rate constant of $1.6 \cdot 10^{12} \text{ cm}^3 \text{ mol}^{-1} \text{ s}^{-1}$ at 443 K.

Pilling et al. [4] used flash photolysis of azomethane in a quartz reaction vessel to study minor products from the pyrolysis of CH_3 radicals. By extrapolation a limiting high pressure rate constant of $1.2 \cdot 10^{12} \text{ cm}^3 \text{ mol}^{-1} \text{ s}^{-1}$ at 298 K was obtained for $\text{CH}_3 + \text{NO}$.

Lifshitz et al. [5] studied the reaction of $\text{CH}_3 + \text{NO}$ behind reflected shock waves in the temperature range between 1100 K and 1300 K. They examined the extent of the HCN production via gas chromatography. For the rate con-

stant they give a value of $k_1 = 10^{11.8} \exp(-62.8 \text{ kJ} \cdot \text{mol}^{-1}/RT) \text{ cm}^3 \text{ mol}^{-1} \text{ s}^{-1}$.

Some more detailed investigations about this reaction up to high temperatures have recently been performed by Frank et al. [6] and by Klatt [7]. They measured profiles of H and of O atoms.

The aim of the present work was to study the formation of H atoms and of HCN in the reaction of $\text{CH}_3 + \text{NO}$ behind incident shock waves by time resolved UV absorption and by IR emission measurements in highly diluted mixtures (10–100 ppm) and under careful control of the NO concentrations present in the mixture.

Experimentals

The measurements of the HCN profiles were performed in an aluminium shock tube with a diameter of 20 cm described in [8], the H atom profiles were taken in a stainless steel shock tube of 8 cm diameter described in [9].

H atoms were monitored by H-ARAS at 121.6 nm with a microwave discharge lamp as light source. The optical setup for the H-ARAS measurements is given in [10]. The calibration was repeatedly checked leading to a calibration curve that slightly differs from that given in [9]. The detection limit for the H atom measurements was better than $1 \cdot 10^{-12} \text{ mol/cm}^3$.

The formation of HCN was followed by the IR emission of HCN on the ν_3 band at $3.02 \mu\text{m}$ with an detection limit of $5 \cdot 10^{-11} \text{ mol/cm}^3$. The emission was followed using an InSb detector. At a distance of 5 cm to the observation window a cylindrical lens with a focal length of 205 mm and between the detector and the lens a filter for $(3.02 \pm 0.01) \mu\text{m}$ (Fa. LOT) were mounted. The time resolution was better than 10 μs . The system was calibrated for HCN by shock heating HCN/Ar mixtures of known concentration. HCN was synthesised according to the method of Slotta [11].

NO was purified by trapping in acetone/nitrogen and nitrogen until a white solid of pure NO was obtained. The purity of NO was checked using mass spectroscopy. The test gas mixtures were prepared before each experiment using a flow system described in [12] to reach initial concentrations of azomethane of 10 ppm. Only mixtures younger than 7 h were used.

Experimental Results

HCN-Measurements

The IR-emission due to the ν_3 -band of HCN was measured behind incident shock waves in the temperature range between 1300 K and 2080 K at total densities varied around $3 \cdot 10^{-6} \text{ mol/cm}^3$. The gas mixtures contained 100 ppm azomethane or less and around 2% NO. With either azomethane or NO alone present in the shocked gas no IR signal was obtained in the wavelength interval used.

The IR signals start to rise after passage of the shock front within their time resolution. They rise further and reach after about 100 μs , depending on experimental conditions, a stationary value.

After converting the signals, using the calibration curves of Fig. 1 and assuming that no other species emit in that wavelength range, the signals could be evaluated towards longer reaction times and for their time behaviour.

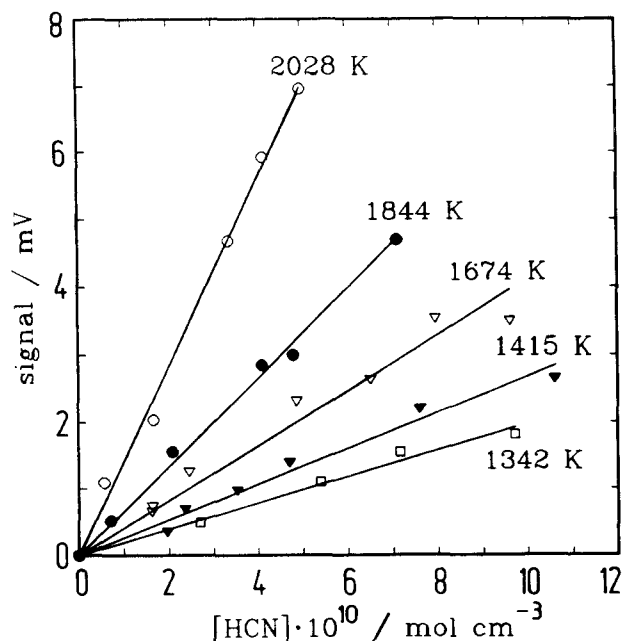


Fig. 1
Calibration curves for emission of HCN

For the evaluation of the reaction rate the truncated mechanism given in Table 2 was used and the simulation was performed with the code of Warnatz [13]. For the fitting the rate constants of the reactions 1 and 2 were varied.

Table 1
Experimental data

Exp. No.	T K	$10^6 \rho$ $\text{mol} \cdot \text{cm}^{-3}$	P mbar	$k_1 \cdot 10^{-10}$ $\text{cm}^3 \text{mol}^{-1} \text{s}^{-1}$	$k_2 \cdot 10^{-09}$ $\text{cm}^3 \text{mol}^{-1} \text{s}^{-1}$	$k_{\text{ges}} \cdot 10^{-10}$ $\text{cm}^3 \text{mol}^{-1} \text{s}^{-1}$
HCN01	1316	4.41	483			9.8
HCN02	1412	3.84	451			10.0
HCN03	1522	3.42	433			12.0
HCN04	1626	4.00	541			13.1
HCN05	1735	3.63	524			15.0
HCN06	1815	3.39	512			13.2
HCN07	1900	3.24	512			17.1
HCN08	2073	2.76	476			29.9
H01	1323	7.65	842	0.60	0.55	0.65
H02	1456	6.52	789	1.15	1.00	1.25
H03	1479	2.60	812	1.12	1.64	1.28
H04	1583	5.45	717	1.44	2.45	1.68
H05	1620	5.31	715	2.13	3.00	2.43
H06	1863	5.46	846	3.43	8.00	4.23
H07	1903	4.79	792	3.77	8.30	4.60
OH1	1502	2.82	352	1.29	1.12	1.40
OH2	1683	2.79	391	2.26	3.02	2.56
OH3	1773	2.52	372	2.86	4.47	3.31
OH4	1934	2.23	359	4.31	6.31	4.94
OH5	2033	2.02	341	5.98	12.6	6.11

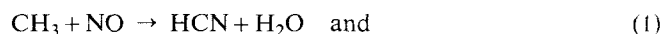
Some of the data are shown in Table 1. The values of the reaction rate constants evaluated from the signals look rather high. However, as in other cases, this could be due to the formation of vibrationally excited HCN in the reaction which can lead to rate constants which seem to be too high [14].

The important point here is the observation that the HCN yield referred to the CH_3 -initial concentration is always close to 100% after longer reaction times. At these times intermediates should have been disappeared. Other possible products, that means long living reaction products like CH_2O , H_2O , NH_3 or CO [14], should not contribute essentially in the wavelength range used here.

It is therefore concluded that HCN is a main product of the reaction of CH_3 with NO at high temperatures. This agrees well with the results from Lifshitz [5].

H-Measurements

Assuming that the reaction of CH_3 with NO at high temperatures leads mainly to



H atoms should arise from the dissociation of CH_2N . A single step to $\text{HCN} + \text{H} + \text{OH}$ would require a rather high activation energy. Other possible H forming channels (in secondary reactions [2]) proceed via CO containing species which can hardly be converted into HCN under our conditions. Therefore the assumption does not seem to be unreasonable.

Lyman- α -absorption experiments were performed in the temperature range between 1300 K and 1900 K behind incident shock waves. The total densities and the azomethane concentrations were around $(5 \pm 3) \cdot 10^{-6} \text{ mol/cm}^3$ and $(8 \pm 3) \cdot 10^{-11} \text{ mol/cm}^3$, respectively.

The H absorption signals start to rise, after a short induction time due to reaction 2a with $k_{2a} = 3 \cdot 10^{14} \exp(-92 \text{ kJ/mol}/RT) \text{ s}^{-1}$ [15] and reach a plateau after about 400 μs . The background absorption of NO at Lyman α , which was approximately constant during the experiment was considered by an expression for the NO-absorption coefficient $\sigma^{121.5 \text{ nm}}$ of

$$\sigma^{121.5 \text{ nm}} = (8.794 \cdot 10^{-19} + 1.150 \cdot 10^{-21} \cdot T/\text{K}) \text{ cm}^2 .$$

After converting the absorption signals into concentration profiles, the profiles were evaluated by computer simulation with the mechanism given in Table 2 by varying k_1 and k_2 . Fig. 2 shows a typical H-concentration profile with a computer simulation. The solid line represents the calculated, the dashed line the measured concentration profile. The contribution of channel 2 was in these measurements around 20–25% of the main channel. Some data are given in Table 1 and in Fig. 3 (open symbols).

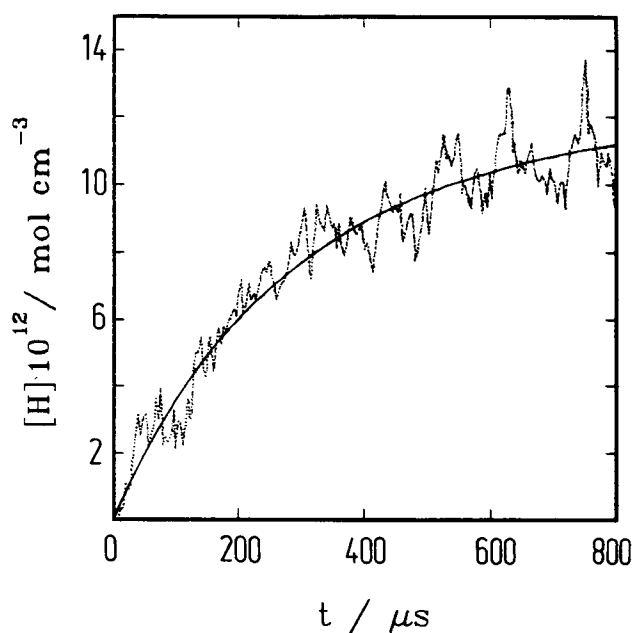


Fig. 2
H-concentration time profile of H05 at $\lambda = 121.5 \text{ nm}$, $T_2 = 1620 \text{ K}$, $\rho_2 = 5.31 \text{ mol cm}^{-3}$, 11.4 ppm azomethane and 1% NO, --- experimental profile, — simulated profile

Table 2
Reaction mechanism^{a)}

No.	Reaction	$\log A$	b	E_a	Ref.
(1)	$\text{CH}_3 + \text{NO} \rightarrow \text{HCN} + \text{H}_2\text{O}$		this work		
(2)	$\text{CH}_3 + \text{NO} \rightarrow \text{CH}_2\text{N} + \text{OH}$		this work		
(3)	$\text{CH}_3 + \text{OH} \rightarrow \text{CH}_3\text{O} + \text{H}$	11.7		0.0	est ^{b)}
(4)	$\text{CH}_3 + \text{OH} \rightarrow {}^1\text{CH}_2 + \text{H}_2\text{O}$	12.5		0.0	est ^{b)}
(5)	$\text{HCN} + \text{H} \rightarrow \text{H}_2 + \text{CN}$	14.6		103.0	[19]
(6)	$\text{NO} + \text{H} \rightarrow \text{N} + \text{OH}$	14.4		211.0	[20]
(7)	$\text{C}_2\text{H}_6 + \text{H} \rightarrow \text{C}_2\text{H}_5 + \text{H}_2$	2.7	3.5	21.8	[21]
(8)	$\text{C}_2\text{H}_6 + \text{OH} \rightarrow \text{C}_2\text{H}_5 + \text{H}_2\text{O}$	6.8	2.0	2.7	[21]
(9)	$\text{C}_2\text{H}_5 + \text{M} \rightarrow \text{C}_2\text{H}_4 + \text{H} + \text{M}$	17.0		130.0	[21]
(10)	$\text{C}_2\text{H}_4 + \text{H} \rightarrow \text{C}_2\text{H}_3 + \text{H}_2$	14.2		43.7	[21]
(11)	$\text{C}_2\text{H}_6\text{N}_2 \rightarrow 2\text{CH}_3 + \text{N}_2$	11.3		140.0	[22]
(12)	$\text{CH}_3 + \text{CH}_3 \rightarrow \text{C}_2\text{H}_6$	11.3		-29.8	[22]
(13)	$\text{CH}_3 + \text{CH}_3 \rightarrow \text{C}_2\text{H}_5 + \text{H}$	13.4		56.9	[23]
(14)	$\text{CH}_3 + \text{CH}_3 \rightarrow \text{C}_2\text{H}_4 + \text{H}_2$	12.8		69.0	[23]
(15)	$\text{CH}_3 + \text{C}_2\text{H}_6 \rightarrow \text{CH}_4 + \text{C}_2\text{H}_5$	-0.3	4.0	34.7	[21]
(16)	$\text{CH}_3 + \text{H} \rightarrow {}^3\text{CH}_2 + \text{H}_2$	13.9		63.0	[24]
(17)	$\text{CH}_4 + \text{M} \rightarrow \text{CH}_3 + \text{H} + \text{M}$	17.3		370.0	[21]
(18)	$\text{CH}_4 + \text{H} \rightarrow \text{CH}_3 + \text{H}_2$	4.3	3.0	36.6	[25]
(19)	${}^1\text{CH}_2 + \text{NO} \rightarrow \text{HCN} + \text{OH}$	14.2	-1.4	0.0	[26]
(20)	$\text{CH}_3\text{O} + \text{H} \rightarrow \text{CH}_2\text{O} + \text{H}_2$	13.3		0.0	[21]
(21)	$\text{CH}_3\text{O} + \text{M} \rightarrow \text{CH}_2\text{O} + \text{H} + \text{M}$	14.4		83.0	[27]
(22)	$\text{CH}_2\text{N} + \text{M} \rightarrow \text{HCN} + \text{H} + \text{M}$	14.5		92.0	[15]
(23)	$\text{CH}_4 + \text{OH} \rightarrow \text{CH}_3 + \text{H}_2\text{O}$	6.2	2.1	10.3	[21]
(24)	$\text{CH}_2\text{O} + \text{OH} \rightarrow \text{CHO} + \text{H}_2\text{O}$	9.5	1.2	2.7	[21]
(25)	$\text{CH}_2\text{O} + \text{H} \rightarrow \text{CHO} + \text{H}_2$	13.4		16.7	[21]
(26)	$\text{CHO} + \text{M} \rightarrow \text{CO} + \text{H} + \text{M}$	14.0		10.0	[21]
(27)	$\text{OH} + \text{H} \rightarrow \text{H}_2\text{O}$	17.9	-2.0	0.0	[21]
(28)	$\text{OH} + \text{OH} \rightarrow \text{H}_2\text{O} + \text{O}$	9.2	1.1	31.6	[21]
(29)	$\text{O} + \text{H}_2 \rightarrow \text{OH} + \text{H}$	7.2	2.0	31.6	[21]
(30)	$\text{H}_2 + \text{OH} \rightarrow \text{H} + \text{H}_2\text{O}$	8.0	1.6	13.8	[21]
(31)	$\text{H}_2 + \text{M} \rightarrow \text{H} + \text{H} + \text{M}$	14.3		402.0	[21]

^{a)} Rate constants are given in terms of $k = A \cdot T^b \cdot \exp(-E_a/RT)$. Units are K, cm^3 , mol, kJ.

^{b)} Estimated.

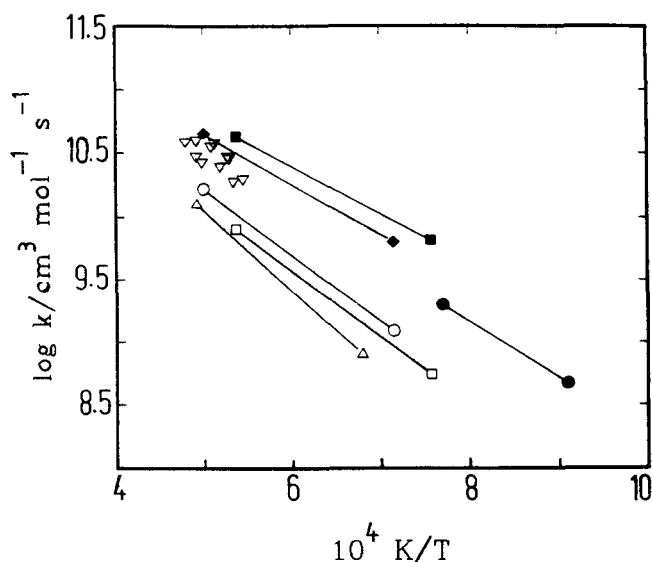


Fig. 3
Rate constants for the reaction $\text{CH}_3 + \text{NO}$; ● Lifshitz (k_{ges}), ◆ Frank et al. (k_{ges}), ■ this work (k_{ges}), ○ Frank et al. (channel 2 from H-atom measurements), □ this work (channel 2 from H-atom measurements), △ Hoffmann et al. reevaluated (channel 2 from OH measurements), ▽ Wolff (k_{ges} from CH_3 profiles)

The rate constant for the reaction $\text{CH}_3 + \text{NO}$ can be approximated by expressions like $k_{\text{ges}} = (4.0 \pm 0.8) \cdot 10^{12} \exp(-8500 \pm 500 \text{ K}/T) \text{ cm}^3 \text{ mol}^{-1} \text{ s}^{-1}$ for the overall reaction. For the reaction 1, $k_1 = (2.4 \pm 0.4) \cdot 10^{12} \exp(-7900 \pm 400 \text{ K}/T) \text{ cm}^3 \text{ mol}^{-1} \text{ s}^{-1}$ and for reaction 2, the OH formation, $k_2 = (5.2 \pm 0.9) \cdot 10^{12} \exp(-12200 \pm 700 \text{ K}/T) \text{ cm}^3 \text{ mol}^{-1} \text{ s}^{-1}$.

OH-Measurements

Hoffmann et al. [16] found in shock wave experiments using an Ar-ion laser pumped cw ring dye laser hydroxyl radicals as a primary product of the reaction in the temperature range from 1470 K to 2040 K. The share of channel 2 was determined to be 40% of the main channel. In these measurements a total rate constant for the reaction of $\text{CH}_3 + \text{NO}$ based on the values of Wolff [17] and Baldwin [18] was used. A new evaluation of the signals obtained in [16] with the overall rate constant given above leads to different rate constants for the OH forming channel. Some of the newly determined rate constants and the experimental conditions are summarised in Table 1. The new rate constants agree quite well with the values obtained for reaction 2 from the H atom profiles as shown in Fig. 3.

OH and H profiles show, that the reaction channel 2 contributes about $(25 \pm 10)\%$ to the total reaction of $\text{CH}_3 + \text{NO}$ at high temperatures.

Discussion

For the reaction $\text{CH}_3 + \text{NO}$ the products H and HCN were experimentally determined in the temperature range

from 1300 to 2080 K and simulated by a reaction mechanism which should contain the important reaction steps. The signals of Hoffmann et al. [16] were reevaluated with the overall rate constant from the H-measurements of this work.

The excess of NO (at least factor 100 to the CH_3 -concentration) was necessary to suppress the methyl radical recombination. So the reactions 1 and 2 play the most important role for the CH_3 -consumption. In a sensitivity analysis of the system the channels 1 and 2 were found to have the biggest influence on the H-concentration profiles of the reaction CH_3 with NO. Other sensitive reactions for the H-concentration profiles are the CH_3 -recombination reactions 12 and 13 forming C_2H_6 and $\text{C}_2\text{H}_5 + \text{H}$.

The IR-emission experiments support the assumption of the two product channels, because the yield of HCN was almost 100% of the initial concentration of CH_3 . But the rate constants from these HCN experiments differ about a factor 10 from the H-measurements. Vibrational relaxation effects of the HCN molecule at the used pressures around 500 mbar should be the reason for this difference as in the case of CO emission in the $\text{CH}_2 + \text{O}_2$ reaction [14]. At higher pressures the difference of the rate constants becomes smaller.

A comparison of the results in this work with the results of previous studies is shown in Fig. 3. It shows that the values for the rate constants from the H-ARAS measurements agree very well with the results from Frank et al. [6]. They examined the formation of H-atoms by H-ARAS at 121.5 nm and the initial concentration of CH_3I , their methyl radical source, by I-ARAS at 145.9 nm. In the investigated temperature range they reported for the rate constants:

$$k_1 = 1.66 \cdot 10^{12} \exp(-8100 \text{ K}/T) \text{ cm}^3 \text{ mol}^{-1} \text{ s}^{-1}$$

$$k_2 = 7.13 \cdot 10^{12} \exp(-12140 \text{ K}/T) \text{ cm}^3 \text{ mol}^{-1} \text{ s}^{-1}$$

They carefully determined channel 2 and evaluated their H-atom profiles also by computer simulation using a mechanism similar to the one used here. In a sensitivity analysis of the system they found channel 2 to be more important to the H-concentration profiles than channel 1.

The values from Klatt [7] for channel 2 are similar to the values from Frank et al. and from this work. The data of Frank and those reported here confirm that the reaction of $\text{CH}_3 + \text{NO}$ follow at high temperatures the reaction mechanism given above.

We are grateful to the DFG for financial support.

References

- [1] H. Singh, Max-Planck-Institut für Strömungsforschung Göttingen, Bericht 104 (1986).
- [2] C. F. Melius, private communication, Sandia National Laboratories, Livermore, California.
- [3] T. A. Titarchuk, A. P. Ballod, N. G. Prokhortseva, and V. Ya. Shten, Kinet. Catal. 15, 1375 (1974).

- [4] M. J. Pilling and J. A. Robertson, *J. Chem. Soc. Faraday Trans. 1* **73**, 968 (1977).
- [5] P. Frank, Th. Just, A. Lifshitz, and C. Tamburu, *J. Phys. Chem.* **97**, 4085 (1993).
- [6] M. Braun-Unkloff, P. Frank, C. Naumann, and K. Wintergerst, *VDI Berichte 1090*, 287 (1993).
- [7] M. Klatt, private communication, Universität Göttingen 1991.
- [8] K. Holzrichter and H. Gg. Wagner, 18th Symp. (Int.) on Comb. 769 (1981).
- [9] M. Klatt, Dissertation Göttingen (1991).
- [10] M. Klatt, M. Röhrig, and H. Gg. Wagner, *Ber. Bunsenges. Phys. Chem.* **95**, 1163 (1991).
- [11] K. H. Slotta, *Ber. Dtsch. Chem. Ges.* **67**, 1028 (1934).
- [12] G. Hennig, M. Röhrig, and H. Gg. Wagner, *Ber. Bunsenges. Phys. Chem.* **97**, 830 (1993).
- [13] J. Warnatz, U. Maas, and P. Deuflhard, Universität Heidelberg, L. R. Petzold, Sandia National Laboratories, Livermore, California 1989.
- [14] Ch. Dombrowsky and H. Gg. Wagner, *Ber. Bunsenges. Phys. Chem.* **96**, 1048 (1992).
- [15] J. A. Miller and C. T. Bowman, *Prog. Energy Combust. Sci.* **15**, 287 (1989).
- [16] A. Hoffmann, S. M. Hwang, H. Gg. Wagner, and Th. Wolff, *Ber. Bunsenges. Phys. Chem.* **94**, 1407 (1990).
- [17] Th. Wolff and H. Gg. Wagner, *Ber. Bunsenges. Phys. Chem.* **92**, 678 (1988).
- [18] A. C. Baldwin and D. M. Golden, *Chem. Phys. Lett.* **55**, 350 (1978).
- [19] D. C. Bauld, J. Duxbury, S. J. Grant, and D. C. Montagne, *Phys. Chem. Ref. Data* **10**, Supp. *1*, 1-1 (1981).
- [20] T. P. Coffee, *Combust. Flame* **65**, 53 (1986).
- [21] J. Warnatz, in: *Combustion Chemistry*, ed. by W. C. Gardiner, Jr., Springer-Verlag, 1984.
- [22] W. Möller, E. Mozhukhin and H. Gg. Wagner, *Ber. Bunsenges. Phys. Chem.* **90**, 854 (1986).
- [23] S. M. Hwang, Dissertation Austin, Texas 1988.
- [24] Th. Just, 13th Symposium on Shock Tubes and Waves 54 (1981).
- [25] P. Roth and Th. Just, *Ber. Bunsenges. Phys. Chem.* **83**, 577 (1979).
- [26] H. H. Carstens, private communication, MPI Göttingen 1994.
- [27] H.-H. Grotheer and S. Kelm, private communication, Inst. für Phys. Chem. der Verbrennung, DLR Stuttgart 1991.

(Received: February 7, 1994)

E 8632